Whole-body F-18 FDG PET for hepatocellular carcinoma patients after interventional treatment

M. F. CHENG, Y. W. WU, K. Y. TZEN, Y. H. HUANG, R. F. YEN

Department of Nuclear Medicine, National Taiwan University Hospital and National Taiwan University College of Medicine, Taipei, Taiwan, E-mail: rfyen@ ha.mc.ntu.edu.tw

Received November 29, 2006

For hepatocellular carcinoma (HCC) patients after primary treatment, conventional anatomical imagings may not be reliable in detecting residual, recurrent or metastatic lesions. The aim of this retrospective study was to evaluate the usability of FDG PET in the follow-up of HCC patients after prior interventional treatments.

The database consisted of 10 male and 2 female (age range, 46-82 years; mean age, 63.4 ± 11.7 years) who had received primary HCC treatments and underwent FDG PET scans at the National Taiwan University Hospital. The accuracy of FDG PET detection was determined by the histopathological results or other clinical evidences afterwards.

Of the 22 lesions, FDG PET studies were able to detect 8 (8/10, 80%) intrahepatic lesions and 8 (8/12, 66.7%) extrahepatic lesions. The lesion based detection rate of FDG PET is 72.7% (16/22). FDG PET was able to detect at least 1 lesion in 11 patients. The 6 false negative lesions in 6 patients include 2 intrahepatic lesions, 1 brain lesion, 1 sphenoid sinus lesion and 2 multiple subcentimeter pulmonary lesions.

FDG PET scan is able to provide valuable auxiliary information for the follow up of HCC patients clinically suspicious of recurrence if their conventional image findings are not unambiguous.

Key words: hepatocellular carcinoma; FDG; positron emission tomography; recurrence; metastases

Hepatocellular carcinoma (HCC) is one of the most common malignancies and has been reported to cause more than a half million deaths annually worldwide [1]. It is one of the leading causes of cancer death in Taiwan as well. Although partial liver resection or hepatic transplantation is the only potentially curable treatment available in early staged HCC, many locally ablative therapies, such as transcatheter arterial chemoembolization (TACE), percutaneous ethanol injection (PEI), radio-frequency ablation (RFA), are implemented for inoperable or recurrent tumors. Early detection of residual or recurrent HCC malignancy is useful in facilitating follow-up treatment to improve outcome and survival.

Transabdominal ultrasonography (US), contrast-enhanced computed tomography (CT) and magnetic resonance imaging (MRI) are the most utilized tools in detecting recurrent HCC at present. These modalities nevertheless have limited interpretation reliability under the following circumstances. The regenerating nodules, fatty infiltration and arteriovenous shunting caused by liver cirrhosis confound the image appearances of US and CT scan and hinder the detection of HCC [2,3]. Moreover, high concentrations of lipiodol in patients previously treated with oily chemoembolization result in artifacts on CT scan and interfere with the differentiation of viable tumor from necrosis [4]. Tumors after TACE are hardly differentiated in MRI due to various signal intensities shown in conventional MRI spin echo T1 and T2 weighted images. As a result, conventional anatomical imaging studies may not be reliably utilized in detecting residual, recurrent or metastatic HCC after primary treatment.

Recently, F-18-fluoro-2-deoxyglucose (FDG) positron emission tomography (PET), a whole-body imaging technology based on glucose metabolism, has been demonstrated to be effective for tumor detection in a variety of malignant diseases. However, it is also known that the overall sensitivity of FDG PET for the detection of hepatocellular carcinoma is low for primary HCC, especially in well-differentiated, low-grade tumors because of low FDG uptake [5-7]. Nevertheless, FDG PET for the detection of extrahepatic metastatic HCC has been reported to be effective [8]. In this study, we

*Corresponding author

evaluated retrospectively the usability of FDG PET in the follow-up of HCC patients who had received prior interventional treatments and were suspicious of recurrence from clinical or biological information. FDG PET scans were performed on these patients because conventional image findings at the times of their suspected recurrences were inconclusive.

Methods

Patients. The database consisted of 12 consecutive HCC patients (2 female and 10 male, age range, 46-82 years; mean age, 63.4 ± 11.7 years) who had received primary HCC treatments and underwent FDG PET scans at the National Taiwan University Hospital because of the revelation of suspicious recurrences/metastases from clinical data or biological tests between August 2001 and September 2004. 10 of the 12 patients (83%) had α-fetoprotein (AFP) level above 20 ng/ml (mean, 3908 ng/ml, range, 11-29261 ng/ml). The conventional imaging results for these 12 patients were not able to locate the recurrent or metastatic foci. All patients except one had liver cirrhosis that likely resulted from chronic HBV, HCV hepatitis or both. HCC were diagnosed for 9 of the 12 patients from their histopathological results. The other 3 patients were diagnosed of having HCC from tumor stains during their hepatic angiographies. These 12 HCC were classified pathologically into 3 grades based on the Edmonson and Steiner classification: well differentiated (grade I), moderately differentiated (grade II), and poorly differentiated (grade III) [9]. These patients then received hepatic resection or tumor enucleation, TACE, RFA, or PEI interventional treatments. Whole-body FDG PET examination was performed for each patient 22 days to 56 months (mean 10.7 months) after his or her last intrahepatic HCC interventional treatment.

Whole-body FDG PET imaging. To perform PET scan, each patient was injected with 370 MBq (10 mCi) of FDG intravenously after a fasting period of 4 hours or longer. The emission data were collected for each patient 45 minutes after the injection using a GE advance PET scanner (GE Medical Systems, Milwaukee, WI). Transmission scans were obtained with a germanium-68 external pin source. From the collected emission data that had been corrected for scatter, random events and dead time, the image was reconstructed by the iterative reconstruction with attenuation correction (IRAC) using the ordered subsets

Table 1. Patients Characteristics, FDG PET Findings and Follow-up Results

Patient	Sex/Age	Pathology Classifications	Duration Between PET scan and last intervention (months)	AFP levels	PET Findings	Follow-up Results
1	M/63	II	56.4	10424	Right hilum lesion	Confirmed by bronchoscopic biopsy
2	M/65	N/A	0.7	1032	Right posterior caudal, liver	Confirmed by follow-up CI
3	M/82	N/A	2.4	130	Right anterior caudal, liver	Confirmed by follow-up CI
4	M/46	III	3.3	29261	Left subphrenic area	Confirmed by follow-up CI
					–	Left lat. Seg. caudal, liver (CT, Gallium scan)
5	M/65	III	4.2	1867	Left lateral seg., liver	Confirmed by follow-up CI
					–	Multiple lung nodules (< 1cm) in chest X-ray (at the same time)
6	M/63	III	1.6	>1000	Multiple lesions in liver	Confirmed by follow-up CI
7	M/48	II	19.8	243	Left proximal humerus	Confirmed by biopsy
					–	Multiple lung nodules (< 1cm) in CT (at the same time)
8	M/64	N/A	17.1	2395	Right posterior cranial, liver	Confirmed by follow-up CI
9	M/66	III	3.5	11	Right posterior caudal, liver	Confirmed by follow-up CI
					–	Left lateral seg, liver
					Right anterior caudal, liver	Confirmed by follow-up CI
					Right upper lung	Confirmed by follow-up CI
					Right paraaortic LNs	Confirmed by biopsy
10	F/80	N/A	9.6	11	Right posterior cranial, liver	Confirmed by follow-up CI
					Right anterior caudal, liver	Confirmed by follow-up CI
					Celiac, paraaortic, paracaval LNs	Confirmed by biopsy
11	F/72	I	N/A	33	–	Sphenoid sinus metastasis by biopsy 2.5 m after PET
12	M/47	II	6.3	490	Right hilum and bilateral lungs	Confirmed by biopsy
					–	Right parieto-occipital brain lesion 3 m after PET

N/A: not applicable; seg.: segment; LN: lymph node; CI: conventional imaging

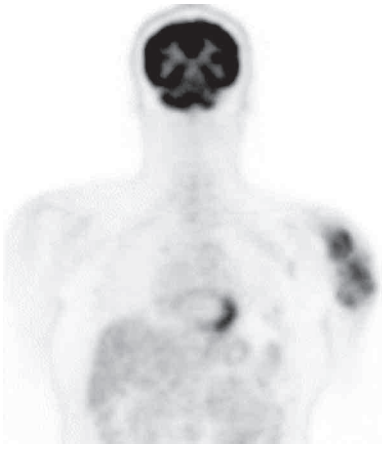

Figure 1. The FDG PET image of a 49-year-old male patient (patient #7) performed 19.8 months after right lobe hepatectomy. Intense FDG uptake was noted in the left proximal humerus. However, the multiple small lung nodules noted in his chest CT were not FDG-avid.

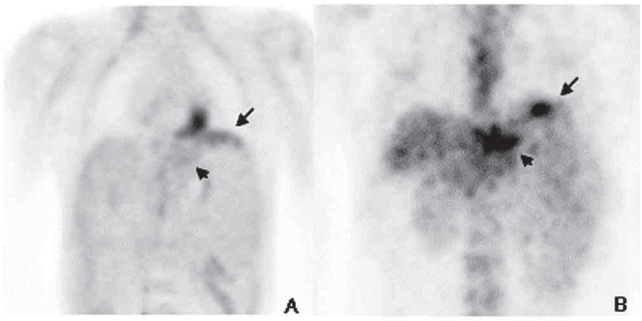

Figure 2. (A) FDG PET image and (B) ^{67}Ga image for a 46-year-old male patient (patient #4). Image (A) shows abnormal FDG uptake in left subphrenic area (arrow) with recurrent viable tumors confirmed by the follow-up CI. The 3 cm lesion in left liver lobe (arrow head) is not observable on image (A). Image (B) reveals increased ^{67}Ga uptake in both arrowed areas.

expectation maximization (OS-EM) algorithm. Image pixel size was 3.0 mm in a 128 × 128 array.

Image interpretation. All the FDG PET images of these 12 HCC patients were interpreted qualitatively by the consensus of two experienced nuclear medicine physicians without prior knowledge of the results of other imaging procedures and follow-up status of these patients. An area with focally accentuated FDG activity that was greater than the activity of the contralateral structure or surrounding tissues was identified as a positive lesion.

Those patients whose PET results were positive were clinically followed up by conventional imaging (CI) or histopathology. It has been reported that the median doubling time of HCC is around 93.5 to 117 days even though tumor growth rate of HCC varies greatly [10,11]. In light of this, patients whose PET results were negative were followed up after their PET studies for at least 3 months by CI. The mean interval between the timing of PET scan and CI was 72 days (range 3-292 days).

Results

The accuracy of this PET study was determined from comparing the PET results with the final clinical data in a lesion-by-lesion manner. The total number of lesions in these 12 HCC patients was clinically confirmed to be 22 (10 intrahepatic and 12 extrahepatic). Table 1 lists patients' characteristics, pathological classifications of primary tumor, AFP levels, PET findings and follow-up results. Among the 22 lesions, FDG PET studies was able to detect 8 (8/10, 80%) intrahepatic lesions and 8 (8/12, 66.7%) extrahepatic lesions. The lesion based detection rate of FDG PET is 72.7% (16/22). FDG PET was able to detect at least 1 lesion in 11 patients. The maximum diameter of FDG-avidity tumors in this study ranged from 0.9~5.2 cm (mean 3.2 cm).

There were six PET false-negative cases in six different patients: two intrahepatic and four extrahepatic. The first two extrahepatic cases were the escapes of the detection of PET in 2 patients for their multiple lung nodules because of small size (< 1cm). The third extrahepatic case was a right parieto-occipital brain lesion noted 3 months later after the patient's PET study. The forth extrahepatic case was a sphenoid sinus metastasis discovered 2.5 months after PET. Except for the patient of the forth extrahepatic case, at least one FDG-avid lesion in each patient was detected by PET scan. The PET images for a 48-year-old male patient (patient #7) with PET positive lesion at left proximal humerus and PET negative lesions in lung are illustrated in Figure 1. Biopsy of the soft tissue mass at his left proximal humerus disclosed malignancy. The multiple small lung nodules revealed in his chest CT were not FDG-avid.

It appeared that there was no definite correlation between the magnitude of FDG uptake and the corresponding serum AFP measurement in this study.

Discussion

We have shown in this study that FDG PET scan for following up HCC patients was able to detect 72.7% lesions that had not been conclusively identified by other conventional imaging methods. In addition, the PET results might discover unexpected metastatic foci and gave rise to additional therapy management.

In the present study, there are 6 PET false-negative cases. In patient #4 and #9, recurrent intrahepatic HCCs were metabolically indistinguishable from the normal hepatic parenchyma despite avid FDG uptake in the extrahepatic sites. Many studies have delineated large variations of FDG accumulation in HCC, probably due to various expressions of glucose-6-phosphatase in tumor cells [5]. Well-differentiated HCC usually has higher glucose-6-phosphatase expression than poorly-differentiated one. Higher glucose-

6-phosphatase activity often brings about less FDG accumulation. As a result, HCC with higher tumor differentiation (lower pathologic grade) generally has less intensity of FDG uptake.

Recently, it has been reported that C-11-acetate yields better sensitivity and specificity as a radiotracer than FDG in resolving low- and intermediate-grade HCC [12,13]. C-11-acetate is a metabolic substrate of β–oxidation. Its mechanism of tumor uptake is believed to be related to the participation of free fatty acid synthesis. The complementary nature of C-11-acetate and FDG in the detection of HCC has already been observed by Ho et al. [12].

It is known that cellular kinetic changes and tumor dedifferentiation may occur within advanced stages of HCC, and glucose transporter protein expression is higher in advanced HCC than that in early HCC [14,15]. It is possible that metastatic tumor cells may enhance their retention of FDG radiotracer and become observable with enough FDG uptakes even though their primary tumors are absent of noticeable FDG uptakes. We believe that these are the circumstances for patent #4 and #9 in this study, their extrahepatic matastaic lesions were PET detectable but their intrahepatic lesions were not.

The PET scan of patient #4 showed the only abnormal FDG uptake in left subphrenic area (Figure 2A). A ^{67}Ga imaging performed one week later confirmed this PET finding but revealed another 3 cm lesion in left liver lobe (Figure 2B). These two areas of recurrent viable tumors were also verified by the follow-up CI. The pathology from a resected HCC before PET scan showed moderately differentiated type (grade II). We have noted that a similar case with negative FDG PET but with positive ^{67}Ga findings in a low-grade HCC was reported by Braga et al. [16]. In our opinion, ^{67}Ga scan is another potential adjunct tool in detecting foci of differentiated HCC.

The two lesions that escaped from PET detection were the one in sphenoid sinus for patient #11 and the other in brain for patient #12. It is well known FDG PET has a blind spot in diagnosing brain malignancies or metastases [17,18]. For patient #11, a 72-year-old female patient who was later clinically confirmed of having metastasis in sphenoid sinus, the standard uptake value (SUV) of FDG in the sphenoid sinus was measured to be only 2.6 while the SUV for the adjacent frontal cortex was 5.2 (Figure 3). The intense FDG activity in the normal cortex of brain prevented us from identifying the abnormal metabolism in sphenoid sinus of patient #11.

Owing to the inherent resolution limit of the PET scanner and respiratory movement, the diffuse pulmonary metastases with sized <1cm in diameter occurred in two patients were not detectable on their PET images even under retrospective study. It is known that nodule visibility on PET scan not only depends on its size and location but also on its intrinsic metabolic activity. We want to point out that a 0.9cm lesion was noted on the abdominal US of patient # 10 with manifested intense FDG uptake (Figure 4).

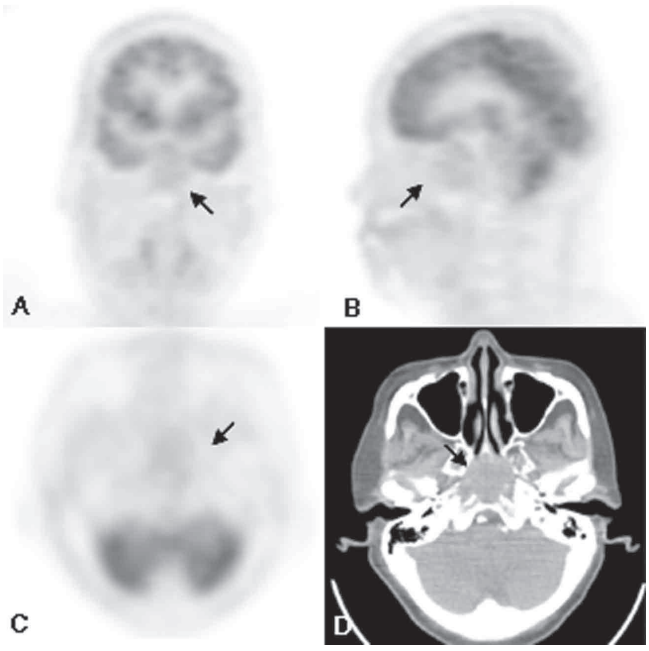

Figure 3. The FDG PET images of a 72-year-old female patient (patient #11) who was confirmed of metastasis in her sphenoid sinus 2.5 months after her PET study. Mild, diffuse FDG uptake with SUV equaled to 2.6 in the sphenoid sinus. This image was diagnosed as PET negative.

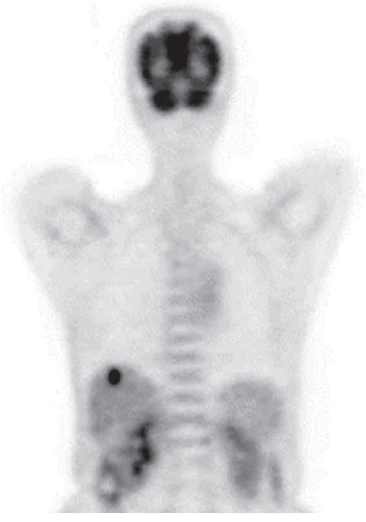

Figure 4. The FDG PET image of an 80-year-old female patient (patient #10) with a lesion of intense FDG uptake at right posterior liver. The lesion size measured by abdominal US was 0.9 cm in diameter.

Most patients in this study had received TACE, PEI or RFA before their PET study. Although CT has been regularly used in the follow-up after therapy, it is of limited value because CT images do not directly display tumor viability.

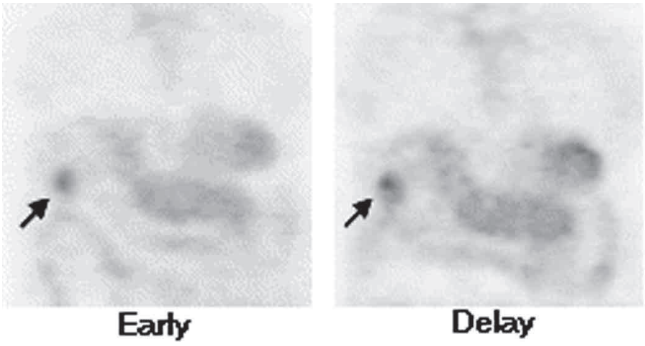

Figure 5. The early and delay FDG PET images for an 82-year-old male patient (patient #3). The tumor at the right liver lobe (arrow) has better lesion/background ratio in the 2h-delay image. This tumor was confirmed in the follow-up angiography.

We have found that FDG-PET is capable of identifying residual viable tumors around the areas of previous intervention. We have also noticed that the additional delayed images, which were performed 2 h after intravenous injection of FDG for a small number of patients in this study, have higher lesion/background ratio than the conventional early images performed 45-60 min after injection (Figure 5). This usefulness of delayed imaging in detecting HCC was also noted previously [19,20].

Study Limitations. Because of limited evidence in the effectiveness of FDG PET in detecting primary, recurrent and metastatic HCC in published references, the costly FDG PET scan, of which the cost is not reimbursed by the national health insurance of Taiwan, is used only when CI finding is inconsistent with the patient's AFP level or clinical symptoms in our center. As a result, there are only a few cases available in this retrospective study (12 patients with 22 lesion sites). Besides, the various timing of CI scans relative to the PET imaging make an across-the-board comparison between different imaging modalities difficult. Still, this study has demonstrated that FDG PET can be an effective adjuvant tool to CI in detecting residual, recurrent or metastatic HCC.

Conclusion

FDG PET scan is able to provide valuable auxiliary information for the follow up of HCC patients clinically suspicious of recurrence if their conventional image findings are not unambiguous. For HCC patients with negative FDG PET results, their lesions are usually of the well-differentiated histology type and additional ^{67}Ga scintigraphy or PET scan using non-FDG radiopharmaceuticals such as C-11-acetate may be capable of identifying the well-differentiated HCC lesions.

The authors acknowledge Mr. Chien-Chung Chen in PET Center, National Taiwan University Hospital, for his technical assistance.

References

[1] EL-SERAG HB. Hepatocellular carcinoma: an epidemiologic view. *J Clin Gastroenterol.* 2002; 35: S72–8.

[2] DODD GD 3RD, MILLER WJ, BARON RL, et al. Detection of malignant tumors in end-stage cirrhotic livers: efficacy of sonography as a screening technique. *Am J Roentgenol.* 1992; 159: 727–33.

[3] COAKLEY FV, SCHWARTZ LH. Imaging of hepatocellular carcinoma: a practical approach. *Semin Oncol.* 2001; 28: 460–73.

[4] SACCHERI S, LOVARIA A, SANGIOVANNI A, et al. Segmental transcatheter arterial chemoembolization treatment in patients with cirrhosis and inoperable hepatocellular carcinomas. *J Vasc Interv Radiol.* 2002; 13: 995–9.

[5] TORIZUKA T, TAMAKI N, INOKUMA T, et al. In vivo assessment of glucose metabolism in hepatocellular carcinoma with FDG-PET. *J Nucl Med.* 1995; 36: 1811–7.

[6] KHAN MA, COMBS CS, BRUNT EM, et al. Positron emission tomography scanning in the evaluation of hepatocellular carcinoma. *J Hepatol.* 2000; 32: 792–7.

[7] TROJAN J, SCHROEDER O, RAEDLE J, et al. Fluorine-18 FDG positron emission tomography for imaging of hepatocellular carcinoma. *Am J Gastroenterol.* 1999; 94: 3314–9.

[8] SUGIYAMA M, SAKAHARA H, TORIZUKA T, et al. ^{18}F-FDG PET in the detection of extrahepatic metastases from hepatocellular carcinoma. *J Gastroenterol.* 2004; 39: 961–8.

[9] EDMONSON HA, STEINER PE. Primary carcinoma of the liver: a study of 100 cases among 48900 necropsies. *Cancer.* 1954; 7: 462–503.

[10] KUBOTA K, INA H, OKADA Y, et al. Growth rate of primary single hepatocellular carcinoma: determining optimal screening interval with contrast enhanced computed tomography. *Dig Dis Sci.* 2003; 48: 581–6.

[11] SHEU JC, SUNG JL, CHEN DS, et al. Growth rate of asymptomatic hepatocellular carcinoma and its clinical implications. *Gastroenterology.* 1985; 89: 259–66.

[12] HO CL, YU SC, YEUNG DW. ^{11}C-acetate PET imaging in hepatocellular carcinoma and other liver masses. *J Nucl Med.* 2003; 44: 213–21.

[13] DELBEKE D, PINSON CW. ^{11}C-acetate. a new tracer for the evaluation of hepatocellular carcinoma. *J Nucl Med* 2003; 44: 222–3.

[14] SASAKI Y, IMAOKA S, ISHIGURO S, et al. Clinical features of small hepatocellular carcinomas as assessed by histologic grades. *Surgery.* 1996; 119: 252–60.

[15] GROBHOLZ R, HACKER HJ, THORENS B, et al. Reduction in the expression of glucose transporter protein GLUT2 in preneoplastic and neoplastic hepatic lesions and reexpression of GLUT1 in late stages of hepatocarcinogenesis. *Cancer Res.* 1993; 53: 4204–11.

[16] BRAGA FJ, FLAMEN P, MORTELMANS L, et al. Ga-67-positive and F-18 FDG-negative imaging in well-differentiated hepatocellular carcinoma. *Clin Nucl Med.* 2001; 26: 642.

[17] LARCOS G, MAISEY MN. FDG-PET screening for cerebral metastases in patients with suspected malignancy. *Nucl Med Commun.* 1996; 17: 197–8.

[18] BRINK I, SCHUMACHER T, MIX M, et al. Impact of [^{18}F]FDG-PET on the primary staging of small-cell lung cancer. *Eur J Nucl Med Mol Imaging.* 2004; 31: 1614–20.

[19] KOYAMA K, OKAMURA T, KAWABE J, et al. The usefulness of ^{18}F-FDG PET images obtained 2 hours after intravenous injection in liver tumor. *Ann Nucl Med.* 2002; 16: 169–76.

[20] LIN YW, TSAI SC, HUNG GU. Value of delayed ^{18}F-FDG PET imaging in the detection of hepatocellular carcinoma. *Nucl Med Commun.* 2005; 26: 31–21.